Macromolecules

Article

pubs.acs.org/Macromolecules

Thiol–Trifluorovinyl Ether (TFVE) Photopolymerization: An On-Demand Synthetic Route to Semifluorinated Polymer Networks

Brian R. Donovan, Jason E. Ballenas, and Derek L. Patton*

School of Polymers and High Performance Materials, The University of Southern Mississippi, Hattiesburg, Mississippi 39406, United States

Supporting Information

ABSTRACT: We report a first example of thiol–trifluorovinyl ether (thiol–TFVE) photopolymerization as a facile, cure-on-demand synthetic route to semifluorinated polymer networks. The thiol–TFVE reaction—which proceeds via anti-Markovnikov addition of a thiyl radial to the TFVE group—was elucidated using model small molecule reactions between phenyl trifluorovinyl ether and thiols with varying reactivity. These model reactions, characterized by ^{19}F NMR, ^{1}H NMR, and FTIR, also provided evidence of an oxygen-induced degradation pathway that may be circumvented by performing the reactions under an inert gas atmosphere. Photopolymerization of difunctional TFVE monomers with multifunctional thiols occurred with rapid kinetics and high conversions as observed with real-time FTIR and provided homogeneous semifluorinated polymer networks with narrow glass transitions as observed with dynamic mechanical analysis. The semifluorinated ether/thioether linkage incorporated into the polymer network yielded hydrophobic materials with increased and tunable T_g, a 2-fold increase in strain at break, 4-fold increase in stress at break, and more than 5-fold increase in toughness relative to a thiol–ene material composed of a structurally similar hydrogenated ether/thioether linkage. The increased T_g and mechanical toughness are attributed to the higher rigidity, hydrogen-bonding capacity, and stronger carbon–carbon bonds of the semifluorinated ether/thioether relative to the hydrogenated ether/thioether.

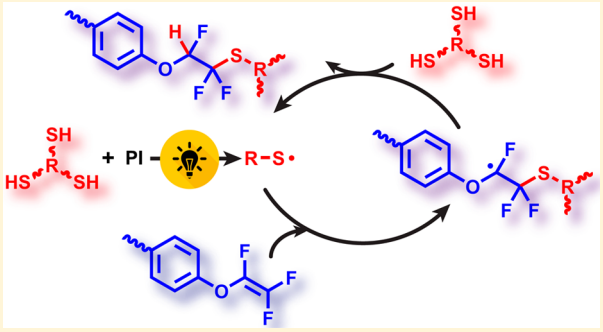

1. INTRODUCTION

Fluorinated polymers have found prolific use in many high performance applications owing to their mechanical strength, high thermal stability, unique optical and electronic properties, low surface energy, and chemical stability.[1−5] While desirable, fully fluorinated polymers are often limited in their application due to their high crystallinity and difficult processing conditions. Hence, many contemporary synthetic efforts are focused on synthesizing amorphous semifluorinated polymers that exhibit analogous properties to fully fluorinated polymers but with improved processability. Of the reported approaches, the use of the trifluorovinyl ether (TFVE) group to synthesize perfluorocyclobutane polymers has provided an effective route to high-performance semifluorinated polymers and polymer networks.[6−9] The TFVE group undergoes a thermally induced [2 + 2] cyclodimerization reaction to form fully amorphous step-growth polymers with improved processability while maintaining the advantageous properties of fluoropolymers. Further, owing to the unique mechanism of TFVE synthesis from phenolic species, a broad library of TFVE-containing monomers can be synthesized under mild conditions with diverse chemical structure.[10,11] With a host of potential monomers available, the TFVE group provides a unique opportunity to synthesize semifluorinated polymers with tunable and distinct macromolecular properties.[6,12−20] Albeit successful in the design and synthesis of semifluorinated polymers, the TFVE cyclodimerization reaction requires high temperatures, long reaction times, and, in some instances, solvent and postpolymerization purification.[7,8,15,16] By contrast, light-mediated polymerizations offer several advantages over thermal polymerizations including shorter reaction times, solvent-free polymerization conditions, lower energy consumption, and both spatial and temporal control over polymerization; however, photopolymerization routes involving TFVE monomers have not been reported. As such, we sought a method to synergistically combine the structural diversity provided by TFVE monomers with the benefits of photopolymerization. In this direction, we were inspired by the early work of Harris and Stacey that reported the efficient addition of the trifluoromethanethiyl radical across a trifluorovinyl methyl ether in the presence of UV irradiation.[21] It is particularly noteworthy that the addition of trifluoromethanethiol proceeded in 15 min (compared to hours or days for other fluorinated olefins) and occurred at the difluorinated, or "tail", carbon only (e.g., anti-Markovnikov addition). Subsequent work demonstrated that hydrogen sulfide, in the presence of X-

Received: August 24, 2016
Revised: September 29, 2016
Published: October 6, 2016

DOI: 10.1021/acs.macromol.6b01822
Macromolecules 2016, 49, 7667−7675

ray or UV irradiation, also undergoes radical addition to a trifluorovinyl methyl ether, and while a 2:1 SH:vinyl ether adduct could be formed, only anti-Markovnikov addition was observed.[22] These results suggest that the TFVE group may be an ideal candidate for photopolymerization, where our interests are specifically the thiol−ene photopolymerization.

Thiol−ene photopolymerizations proceed via a radical step-growth mechanism, where a thiyl radical, formed by hydrogen abstraction from a photoinitiator, adds across a double bond to form a carbon-centered radical. The carbon-centered radical then undergoes an efficient and rapid chain transfer reaction with an additional thiol to generate the thiol−ene product and regenerate the propagating thiyl radical species. The radical step-growth nature of the polymerization mechanism imparts several unique advantages to the synthesis of polymer networks including rapid polymerization times, high conversions, insensitivity to oxygen, and homogeneous network structure characterized by uniform and tailorable thermal and mechanical properties.[23,24] Few examples of semifluorinated thiol−ene materials have been reported in the literature,[25−27] and these examples all employ monomers containing semifluorinated pendent groups. Herein, we demonstrate a first example of thiol−trifluorovinyl ether (thiol−TFVE) photopolymerization as a facile, cure-on-demand synthetic route to semifluorinated polymer networks. The thiol−TFVE reaction was initially elucidated using model small molecule reactions between phenyl trifluorovinyl ether and thiols with varying reactivity. Photopolymerization of difunctional TFVE monomers with multifunctional thiols was assessed in terms of polymerization kinetics, while the mechanical and thermomechanical properties of the resulting semifluorinated networks were systematically characterized as a function of TFVE concentration.

2. RESULTS AND DISCUSSION

2.1. Model Thiol−TFVE Reactions. The thiol−TFVE reaction was initially investigated using model reactions between phenyl trifluorovinyl ether (Ph−TFVE) and a series of thiols of increasing reactivity (methyl 3-mercaptopropionate [M3MP] > 1-propanethiol [PrSH] > benzyl mercaptan [BnSH]),[23] as shown in Figure 1. TFVE, thiol, and photoinitiator were combined without solvent and exposed to UV light (100 mW/cm^2) in air. The structure of the thiol−TFVE adduct was characterized using ^{1}H and ^{19}F NMR. Figure 2 shows the ^{1}H and ^{19}F NMR spectra for the M3MP/Ph−TFVE adduct (see Figures S1−S9 for NMR of other adducts). In each reaction, the thiol successfully added across the TFVE

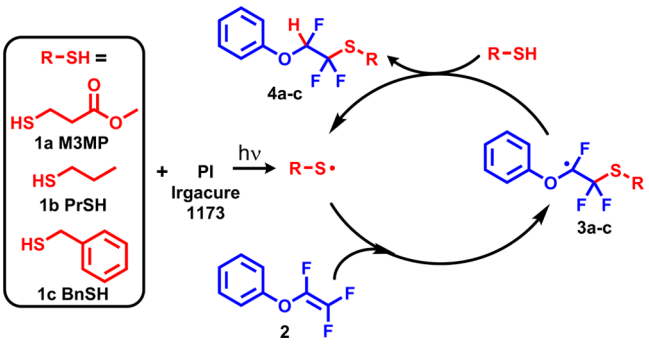

Figure 1. Model reaction between Ph−TFVE and a series of thiol monomers with increasing reactivity in the order M3MP > PrSH > BnSH.

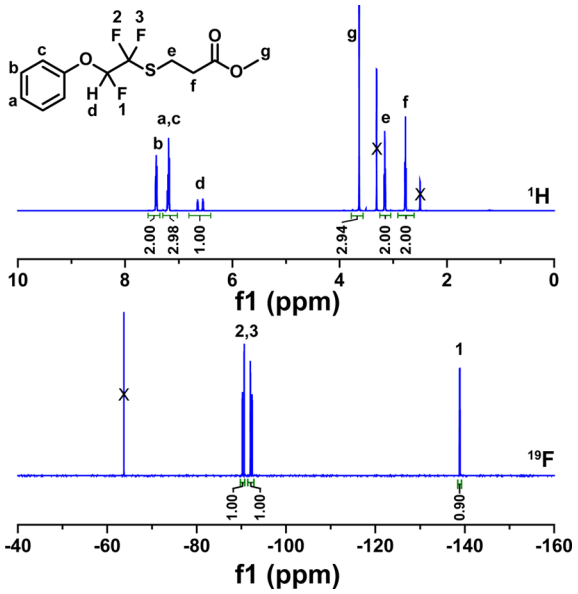

Figure 2. ^{1}H NMR (top) and ^{19}F NMR (bottom) of M3MP/Ph−TFVE addition adduct.

functional group to afford a semifluorinated ether/thioether linkage. Control experiments conducted with M3MP/Ph−TFVE in the absence of photoinitiator and UV light revealed no reaction after 5 days (Figure S10), suggesting the thiol addition does not proceed through charge transfer or co-oxidation reactions.[28] The appearance of a single proton peak, **d**, centered around 6.50 ppm represents the hydrogen on the carbon alpha to the ether linkage, previously a part of the thiol functional group. Additionally, ^{19}F NMR reveals the disappearance of the TFVE group and the formation of two doublets of doublets of doublets (ddd) and a doublet of triplets (dt), representing fluorines **1** and **2**, and **3**, respectively. The anti-Markovnikov addition product was confirmed by the close inspection of the fluorine peak splitting patterns. The ddd peaks have splitting patterns with J values of approximately 225, 13, and 3 Hz corresponding to geminal F−F splitting, vicinal F−F splitting, and vicinal H−F splitting, respectively (see Figure S11). The dt peak has splitting patterns with J values of approximately 59 and 14 Hz corresponding to geminal H−F splitting, and vicinal F−F splitting, respectively. The splitting patterns and associated integration values confirm the anti-Markovnikov addition of thiols to the TFVE.

Thiol−ene reactions are typically characterized by rapid reaction rates, high conversions, and an insensitivity to oxygen. Figure 3a shows the reaction kinetics between small molecule thiols and Ph−TFVE in air under UV light (1 wt % photoinitiator, 100 mW/cm^2). As expected, the reaction rates follow the order of thiol reactivity with M3MP, PrSH, and BnSH reaching 92%, 70%, and 15% conversion, respectively, within 1 min. TFVE conversion values at 30 min follow a similar trend with M3MP reaching 99% conversion, while PrSH and BnSH reach 87% and 70%, respectively. The thiol−TFVE reactions, when conducted in air, also exhibit a change in color from clear to orange, as shown in inset of Figure 3a. The thiol−TFVE reactions were further investigated under an inert nitrogen atmosphere (1 wt % photoinitiator, 100 mW/cm^2), and the conversion versus time plots are presented in Figure 3b. In all cases, increases in both the initial reaction rates and final conversion values under nitrogen were observed. M3MP and

DOI: 10.1021/acs.macromol.6b01822
Macromolecules 2016, 49, 7667−7675

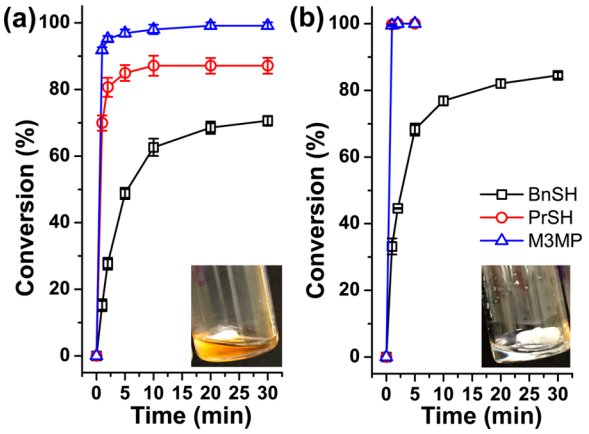

Figure 3. TFVE conversion kinetics for thiol/Ph−TFVE reactions conducted at 1 wt % photoinitiator and 100 mW/cm^2 UV light in (a) air and (b) N_2. Data points represent the average of multiple runs; error bars represent ±1 std dev.

PrSH approached quantitative conversion in approximately 1 min, whereas BnSH showed a 15% increase in overall conversion (from 70% in air to 85% in nitrogen). Thiol−TFVE reactions carried out under nitrogen also remained colorless (Figure 3b, inset). It is worth noting that Ph−TFVE is difficult to homopolymerize under radical conditions.[29] Unsurprisingly, TFVE homopolymerization was not observed under our reaction conditions (Figure S12), indicating that TFVE consumption is solely a function of thiol addition. Changes in photoinitiator concentration improved conversions in both air and nitrogen atmospheres, but BnSH−TFVE reactions in air still failed to reach quantitative conversion (see Figure S13). As a final control experiment, we ran the BnSH−TFVE reaction under UV exposure in an inert atmosphere and in the absence of photoinitiator. Under these conditions, the BnSH−TFVE reaction reached ~40% conversion (Figure S13) and can be attributed to UV-induced cleavage of thiol into thiyl radicals, resulting in photoinitiation (a common result for thiol−ene photoreactions[30]). The absence of Irgacure precludes the possibility of Irgacure serving as a base in the reaction.[31,32] The combined results of these experiments suggest that the SH−TFVE reaction proceeds via a radical addition pathway.

The differences between the kinetic results in nitrogen and air suggest that the thiol−TFVE reaction shows an increased sensitivity to oxygen. As such, we propose the oxygen induced degradation mechanism shown in Figure 4a. Traditionally, when oxygen interacts with the carbon-centered radical formed during the propagation step of the radical thiol−ene reaction, the formed peroxide radical can still participate in polymerization by removing the easily abstractable hydrogen of the thiol group, regenerating the propagating thiyl radical (equivalent to steps 1−3 in Figure 4a).[23,33] In the case of the thiol−TFVE reaction, it appears that oxygen not only inhibits the reaction but may also provide a pathway for product degradation (discoloration). Suspecting oxygen-induced degradation, two additional considerations are made. The first is that the hydroperoxide group formed after the reaction of the carbon-centered radical intermediate with oxygen can recleave to generate oxygen centered radicals (step 4 in Figure 4a).[34−36] The second is that main chain fluoropolymers, and more specifically perfluoroethers, can undergo β-scission when the propagating radical contains an α ether linkage[37] as well as several similar scission pathways when exposed to intense irradiation (step 5 in Figure 4a).[38,39] Steps 4 and 5 present a mechanistic pathway for the decomposition of the formed hydroperoxide and the subsequent and spontaneous scission of the addition product to form an acyl fluoride (**I**) and the stable phenoxyl radical (**II**). The phenoxyl radical and acyl fluoride then hydrolyze in atmosphere (step 6) to yield the final decomposition products, **III**, **IV**, and **V**. Unfortunately, small molecule separations and isolations of the degradation products were difficult and prevented quantitative determination of degradation product structure. However, spectroscopic techniques provided insight into the presence of the proposed

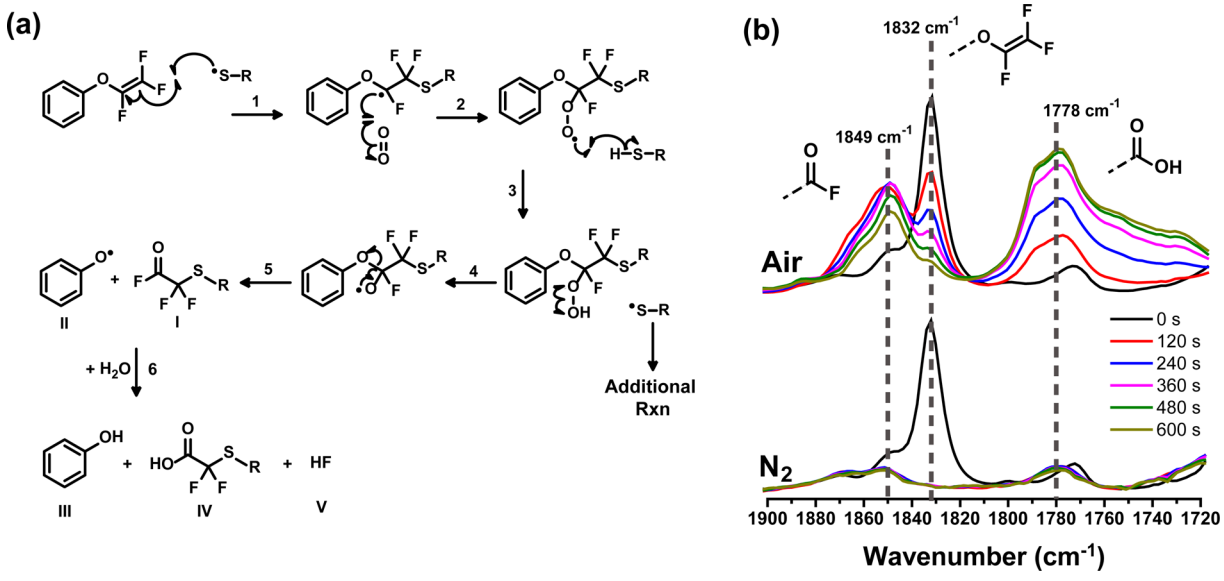

Figure 4. (a) Proposed mechanism for oxygen-induced degradation pathway of thiol/TFVE radical reaction. (b) FTIR spectrum presented at 2 min intervals for the reaction of 1-dodecanethiol/Ph−TFVE 1 wt % photoinitiator upon exposure to 20 mW/cm^2 UV light in air (top) and N_2 (bottom). Radical−radical termination reactions (e.g., disulfide formation and head-to-head coupling of carbon-centered radicals) common to thiol−ene reactions are not shown in the reaction scheme.

DOI: 10.1021/acs.macromol.6b01822
Macromolecules 2016, 49, 7667−7675

carbonyl containing degradation products. As such, a reaction between 1-dodecanethiol and phenyl trifluorovinyl ether in the presence of 1 wt % photoinitiator and 20 mW/cm^2 UV light was conducted over 10 min and monitored in real time using FTIR under both air and nitrogen atmospheres (1-dodecanethiol was used to limit volatility issues and prevent spectral overlap of functional groups). The results of the RT-FTIR study are shown in Figure 4b. From Figure 4b, it is clear that in air the slow disappearance of the TFVE peak at 1832 cm^{-1} is accompanied by the appearance of two distinct peaks centered at 1778 and 1849 cm^{-1}. These peaks are associated with the products of the oxygen degradation mechanism and are noticeably absent when the reaction is conducted in a nitrogen atmosphere. The peak centered at 1778 cm^{-1} is commonly identified with the carbonyl moiety of a carboxylic acid functional group and as such is assigned to the formation of the stable degradation product, **IV**. The peak at 1849 cm^{-1} appears in a region associated with acyl fluorides[40] and is assigned to the formation of degradation product, **I**, in good agreement with literature values for $-SCF_2COF$ IR absorptions.[41] It is also worth noting that the intensity of the −COF peak quickly increased, before decreasing at longer times. The quick appearance of −COF followed by its disappearance coupled with the continuous formation of −COOH can be explained by the hydrolysis of the acyl fluoride, **I**, to the carboxylic acid, **IV**, as shown in step 6 of Figure 4a. Furthermore, two distinct singlets at −83.2 and −83.6 ppm are displayed in the ^{19}F NMR spectrum of the product mixture in air, in agreement with literature values for the chemical shifts of CF_2 fluorines adjacent to carbonyl carbons (Figure S14).[41,42] The CF_2 peaks were not observed by ^{19}F NMR for reactions conducted under N_2.

After identifying the oxygen-sensitive nature of the thiol−TFVE photoreaction, subsequent experiments were conducted under nitrogen. Given the electron deficiency of the TFVE group, the kinetics and efficiency of the thiol−TFVE reaction were somewhat unexpected. To provide a point of reference, we ran the thiol−TFVE reaction parallel to thiol−ene reactions that employ more traditional electron-rich alkenes, such as norbornene, vinyl ether, allyl ether, and allyl groups, and the results are shown in Figure 5. BnSH, as the least reactive thiol of the series, was chosen for the alkene comparison experiment to enable facile capture of the kinetics. In each case, BnSH and the alkene were combined in the absence of solvent with 1 wt % photoinitiator and reacted in an inert N_2 atmosphere for 30 min under 100 mW/cm^2 UV light intensity. As shown in Figure 5, the TFVE group is less reactive and exhibits slower reaction kinetics with BnSH than norbornene, vinyl ether, and allyl ether. However, TFVE reaction rates with BnSH are comparable to allyl reaction rates, though these reactions do not reach the same final conversions after 30 min. It is noteworthy that the kinetics of thiol−TFVE and thiol−ene reactions are indistinguishable (e.g., quantitative conversions within 1 min) when employing more reactive thiols, such as M3MP and PrSH. The unexpected reactivity of the TFVE group is a function of both the carbon-centered radical intermediate and the lability of the thiol hydrogen. Following the propagation step, the carbon-centered radical sits alpha to the ether linkage which can inductively stabilize the radical,[43] lowering the energy barrier to addition. Following radical addition, the easily abstractable thiol hydrogen facilitates the chain-transfer step and the reaction proceeds as previously described. Encouraged by these results, we next explored the thiol−TFVE reaction for synthesis of semifluorinated polymer networks.

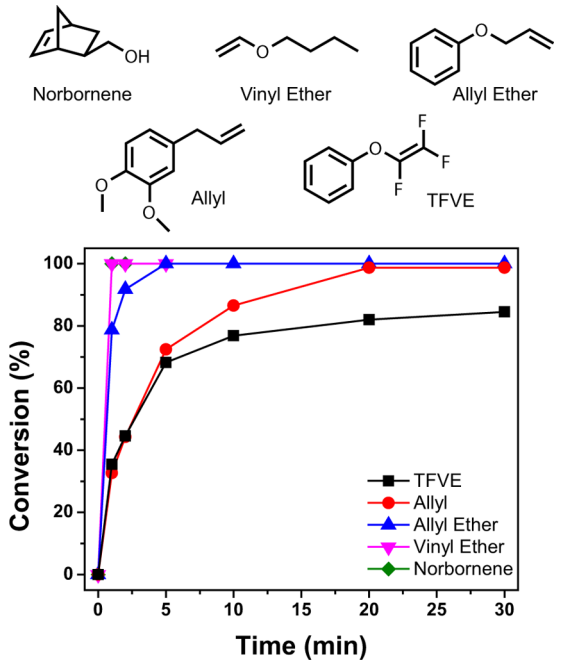

Figure 5. Alkene monomer structures and conversion kinetics for BnSH/alkene reactions conducted at 1 wt % photoinitiator and 100 mW/cm^2 UV light in N_2.

2.2. Semifluorinated Networks. The rapid and efficient reaction kinetics between the TFVE and a variety of thiols make the thiol−TFVE photoreaction an ideal candidate to rapidly synthesize semifluorinated polymer networks with highly tunable properties. Therefore, a difunctional TFVE monomer based on bisphenol A (TFVE-BPA) was synthesized and formulated with di- and trifunctional thiol monomers, as shown Figure 6 (see Figures S15−S22 for NMR spectrum of synthesized difunctional monomers; a 75:25 SH mole ratio of

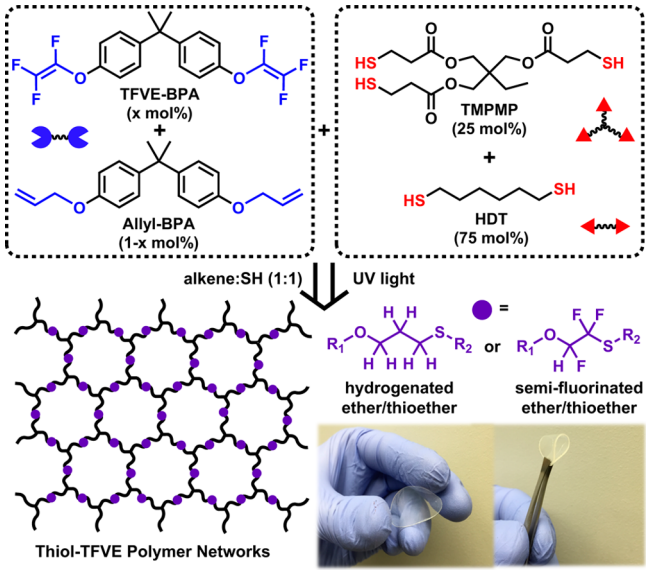

Figure 6. Thiol/TFVE multifunctional network monomers and network preparation. Hydrogenated and semifluorinated ether/thioether linkages are shown in purple.

DOI: 10.1021/acs.macromol.6b01822
Macromolecules 2016, 49, 7667−7675

$HexSH_2$:TMPMP was used to ensure monomer mixture homogeneity). TFVE−BPA was copolymerized with allyl−BPA to tailor the amount of semifluorinated linkages in the network and determine the effect of the TFVE group on the photopolymerization process. The structural similarity of allyl−BPA serves as a control to determine the influence of the semifluorinated linkage on polymer network properties. All formulations contained 1 wt % Irgacure 1173 and were polymerized with 20 mW/cm^2 UV light under an inert N_2 atmosphere. The mol % of TFVE groups was systematically varied from 0 to 100 mol %. The polymerization kinetics as a function of TFVE−BPA concentration are shown in Figure 7.

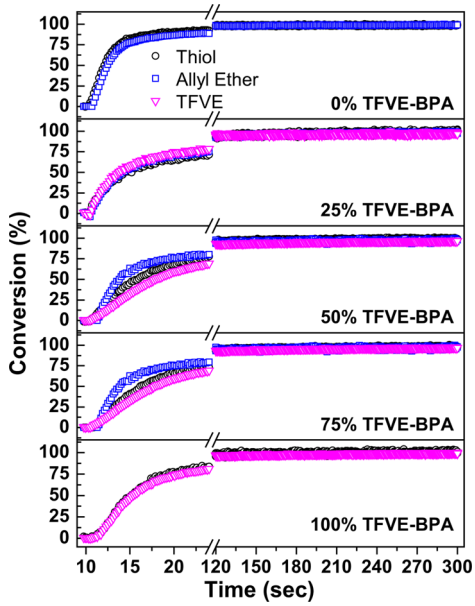

Figure 7. Real-time FTIR conversion plots of thiol/TFVE networks formulated with 0−100 mol % TFVE−BPA.

After 30 s, the 0% TFVE−BPA and 100% TFVE−BPA formulations respectively approached 95% and 85% functional group conversions, while maintaining a 1:1 thiol:alkene stoichiometry throughout the photopolymerization. In copolymerizations of TFVE−BPA and allyl−BPA, the difference in polymerization rate between the allyl ether and the TFVE groups can be observed early in the reaction, with the allyl ether groups reaching an approximately 6% higher conversion than the TFVE groups at 30 s for the 50% and 75% TFVE−BPA formulations. The lower reactivity of the TFVE group in the thiol−ene copolymerization is consistent with the small molecule kinetics presented in Figure 5, as the allyl ether group is a more reactive alkene under the current reaction conditions. However, after 2 min of UV exposure, all network formulations reached near quantitative conversion with stoichiometric conversion of all functional groups. These results confirm that under inert atmosphere semifluorinated networks can be rapidly synthesized and that the TFVE group exerts little to no influence on final conversion values.

The influence of the semifluorinated ether/thioether linkage on the thermomechanical properties of the thiol−TFVE networks was investigated using dynamic mechanical analysis (strain film mode, heating rate 2 °C/min). The glass transition was taken as the peak maximum of the tan δ curves. Figure 8a shows the tan δ curves of the thiol−TFVE networks as a function of TFVE−BPA concentration. At all loadings of

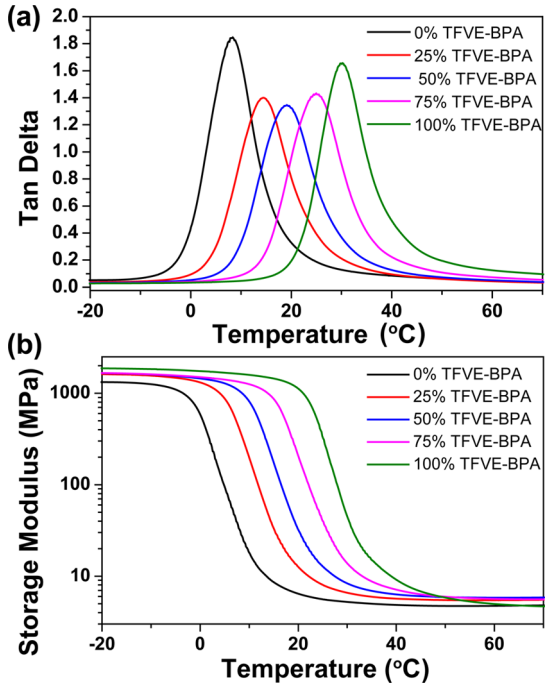

Figure 8. Representative thermomechanical plots of 0−100 mol % TFVE−BPA polymer networks. (a) Tan δ vs temperature. (b) Storage modulus vs temperature.

TFVE−BPA, the tan δ curves exhibit a narrow full width at half-maximum (<13 °C) and are characteristic of homogeneous polymer networks formed via a thiol−ene radical step-growth mechanism.[44] Significant increases in T_g were observed as a function of the semifluorinated ether/thioether linkage, with the T_g increasing from 7.1 ± 1.3 °C, at 0% TFVE, to 29.2 ± 2.3 °C, at 100% TFVE—an increase of more than 20 °C. Interestingly, cross-link densities calculated from the rubbery plateau regions (T_g + 40 °C) of the storage modulus curves (Figure 8b and Table 1) remain relatively constant. Therefore,

Table 1. Thermomechanical Properties of 0−100 mol % TFVE−BPA Thiol/TFVE Polymer Networks

mol % TFVE−BPA	T_g (°C)	fwhm[a] (°C)	ρ_x[b] (mol cm^{-3} 10^3)
0	7.1 ± 1.3	11.2 ± 0.6	0.620 ± 0.023
25	13.8 ± 0.6	11.1 ± 1.3	0.641 ± 0.028
50	18.1 ± 0.9	12.3 ± 0.5	0.664 ± 0.039
75	25.0 ± 1.7	12.3 ± 0.9	0.603 ± 0.071
100	29.2 ± 2.3	10.6 ± 0.2	0.544 ± 0.033

[a]Fwhm obtained from the tan δ curve. [b]Cross-link density.

the observed increases in T_g are a function of the changes in the nature of the cross-links within the backbone of the polymer network. At 0% TFVE−BPA, the radical addition of the thiol to the allyl−BPA results in the flexible ether/thioether linkage (Figure 6). As the allyl−BPA is replaced with TFVE−BPA, the majority of chemical linkages formed within the polymer network are semifluorinated ether/thioethers (Figure 6). The increase in T_g as a function of semifluorinated linkage can be attributed to a combination of factors. The incorporation of fluorine has been shown to increase the rigidity of polymers[45,46] as well as prevent certain modes of rotation through steric and electronic effects.[47] Additionally, the strong electron-withdrawing nature of fluorine is capable of increasing the acidity

DOI: 10.1021/acs.macromol.6b01822
Macromolecules 2016, 49, 7667−7675

of adjacent hydrogen atoms to facilitate hydrogen bonding.[48−50] The incorporation of large amounts of semifluorinated linkages therefore not only stiffens the ether/thioether linkage but also provides a large number of hydrogen bonding sites, which effectively act as physical cross-links.[51] The result is most dramatic when all alkenes are fluorinated, with the T_g of the material transitioning from a flexible rubber (0% TFVE) to a semi-glass-like state (100% TFVE) at room temperature.

The influence of the semifluorinated ether/thioether linkage is also evident in the mechanical properties of the thiol−TFVE networks. Representative stress−strain curves are shown in Figure 9a and summarized in Figure 9b. In general, both stress

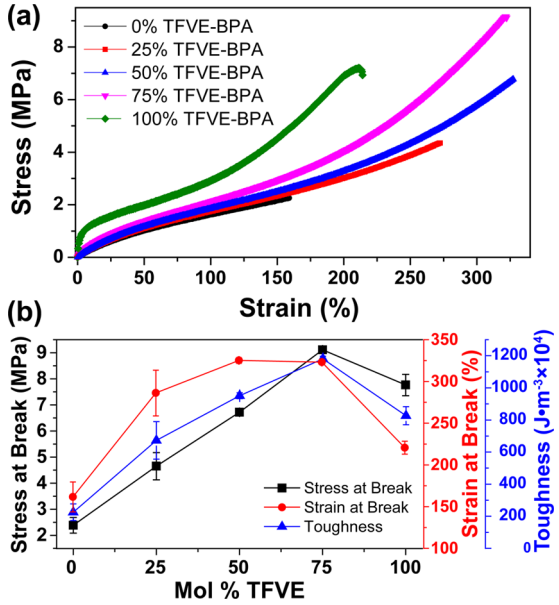

Figure 9. (a) Representative stress/strain curves of 0−100 mol % TFVE−BPA thiol/TFVE networks. (b) Summation of thiol/TFVE polymer network tensile properties as a function of mol % TFVE−BPA. Results indicate a peak in mechanical properties at 75 mol % TFVE−BPA.

at break and strain at break values increased with increasing TFVE−BPA concentration, with the 50−75% TFVE−BPA networks exhibiting a 2-fold increase in strain at break relative to the 0% TFVE−BPA sample. It is also clear that increasing the concentration of semifluorinated linkage within the network results in a 5-fold increase in toughness, peaking at 75 mol % TFVE, relative to the nonfluorinated network (0% TFVE). The 100% TFVE network showed a significant increase in initial modulus; however, a decrease in toughness was observed relative to the 50−75% TFVE samples. The decrease is toughness can be attributed to the more glass-like behavior of the 100% TFVE, as tensile testing was conducted at a temperature (25 °C) just below T_g. The increase in toughness with increasing semifluorinated linkage is attributed to an increase in the bond strength of the chemical cross-links and to the contribution of hydrogen bonding to the absorption of mechanical deformation energy. Because of the inductive effect of fluorine on the skeletal carbon−carbon bonds, the semifluorinated ether−thioether linkage ($HFC-CF_2$) is expected to be stronger than the carbon−carbon bond of the hydrogenated ether−thioether linkage (H_2C-CH_2), which likely translates into an increase in mechanical toughness of the thiol−TFVE network at higher concentrations of TFVE−BPA. Simultaneously, the semifluorinated linkage provides hydrogen bonding sites as physical cross-links that are capable of absorbing the energy of mechanical deformation and rupturing before the covalent cross-links.[52] Ultimately, incorporating semifluorinated ether−thioether linkages via thiol−TFVE photopolymerization provides a facile route to enhance the mechanical properties of thiol−ene polymer networks.

Thermogravimetric analysis was used to characterize the thermal stability of the thiol−TFVE polymer networks. Samples were subjected to a 10 °C/min ramp rate from 30 to 800 °C under a nitrogen atmosphere. Figure 10 shows the

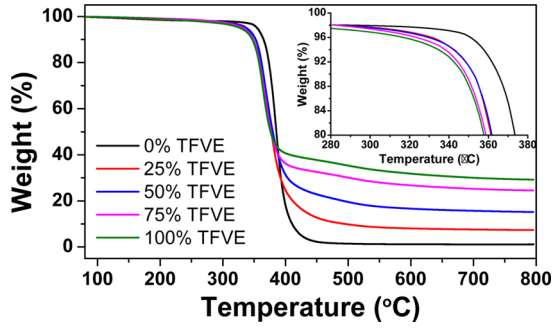

Figure 10. Representative thermal degradation behavior of thiol/TFVE networks in a N_2 atmosphere. The inset shows a more detailed view of the onset region.

TGA thermograms for the thiol−TFVE samples as a function of TFVE−BPA concentration. The data are summarized in Table 2. As illustrated by the 5% weight loss values (T_{d5}%), the

Table 2. Summary of Thermal Degradation Temperatures of Thiol/TFVE Polymer Networks

mol % TFVE−BPA	T_{d5} (°C)	T_{d10} (°C)	1st deriv wt % (°C)	char yield (%)
0	349.9 ± 3.7	359.4 ± 4.0	378.6 ± 4.6	0.7 ± 0.5
25	332.6 ± 3.5	346.9 ± 4.2	365.7 ± 5.0	7.9 ± 0.4
50	332.6 ± 2.9	345.6 ± 4.1	362.9 ± 3.0	16.2 ± 2.6
75	325.2 ± 4.2	342.2 ± 3.7	361.4 ± 3.6	23.6 ± 0.8
100	323.2 ± 3.2	342.1 ± 3.5	359.1 ± 3.6	28.9 ± 1.4

onset of thermal degradation depends on the concentration of semifluorinated ether−thioether in the network, where the highest T_{d5}% was observed for the 0% TFVE−BPA sample. Thiol−TFVE networks containing 25, 50, 75, and 100% TFVE−BPA showed T_{d5}% values respectively at 332.6 ± 3.5, 332.6 ± 2.9, 325.2 ± 4.2, and 323.2 ± 3.2 °C. The decrease in onset of degradation, though minimal between the semifluorinated polymer networks, is significant from the 0% TFVE−BPA network to the 100% TFVE−BPA network (T_{d5}% values shifted ∼30 °C and the first derivative of weight percent values shifted ∼20 °C). The change in thermal degradation behavior for the semifluorinated networks is rationalized by an increase in abstractable hydrogens as more semifluorinated linkage is incorporated into the polymer.[48] Hydrogen abstraction is a common fluoropolymer degradation pathway and may result in the formation of HF, along with the initiation of several radical scission pathways.[38,53] HF thermally released from the polymer has the potential to form inorganic salts leading to an increase in char yield (an advantageous property for fire-resistant materials), as illustrated by the increase from

DOI: 10.1021/acs.macromol.6b01822
Macromolecules 2016, 49, 7667−7675

0.7 ± 0.5% at 0% TFVE−BPA to 28.9 ± 1.4% at 100% TFVE−BPA.

Finally, contact angle measurements show the static water contact angle increases from 95.6 ± 1.6° at 0% TFVE to 101.6 ± 1.6° at 100% TFVE (see Figure S23). The increased hydrophobicity of the networks with increasing TFVE−BPA concentration is attributed to the contribution of the semifluorinated ether/thioether linkage to lower the surface energy—an advantageous property for applications necessitating moisture resistance. The observed contact angles are consistent with other materials reported in the literature that are derived from TFVE-based monomers.[13]

3. CONCLUSIONS

In summary, we have demonstrated the first example of thiol−trifluorovinyl ether photopolymerization as a facile synthetic route to semifluorinated polymer networks. The thiol−TFVE reaction—including anti-Markovnikov addition product and reaction kinetics with various thiols—was elucidated using small molecule model reactions. An oxygen-induced degradation pathway was identified, and a mechanism, supported by NMR and FTIR spectroscopy, was proposed; however, this side reaction was circumvented by performing the reactions under a nitrogen atmosphere. Photopolymerization of difunctional TFVE monomers with multifunctional thiols occurred with rapid kinetics and high conversions and provided homogeneous semifluorinated polymer networks with narrow glass transitions—all hallmark characteristics of the radical step-addition process. Directly incorporating the semifluorinated ether/thioether linkage into the polymer network yielded hydrophobic materials with increased T_g, a 2-fold increase in strain at break, 4-fold increase in stress at break, and more than 5-fold increase in toughness relative to a thiol−ene material composed of a structurally similar hydrogenated ether/thioether linkage. We anticipate that the simplicity and rapid cure kinetics of the thiol−TFVE photopolymerization coupled with on-demand access to tunable and enhanced materials properties will provide a framework for the design of new semifluorinated polymer thermosets for a range of applications.

4. EXPERIMENTAL SECTION

4.1. Materials. All reagents and solvents were purchased from Sigma-Aldrich and used without additional purification unless otherwise specified. Petroleum ether and dichloromethane were purchased from Fisher Scientific; Irgacure 1173 was purchased from BASF; trimethylolpropane tris(3-mercaptopropionate) was purchased from Bruno Bock; and 1,2-dibromotetrafluoroethane and phenyl trifluorovinyl ether (Ph−TFVE) were purchased from SynQuest. Ph−TFVE was further purified by silica gel chromatography prior to use.

4.2. Thiol−TFVE Model Reactions. The following describes a typical thiol−TFVE model procedure: A thiol (methyl 3-mercaptopropionate) (M3MP), 1-propanethiol (PrSH), benzyl mercaptan (BnSH), and phenyl trifluorovinyl ether were combined in a 1:1 SH:TFVE mole ratio in the presence of a small weight percent of photoinitiator (1−3 wt %; Irgacure 1173). The resulting mixture was exposed to 100 mW/cm^2 UV light and monitored by ^{1}H and ^{19}F NMR to determine conversion over time. Reactions conducted in inert atmosphere were subjected to three cycles of freeze−pump−thaw using high purity nitrogen. NMR spectra of purified compounds can be found in the Supporting Information (Figures S1−S9). Chemical shifts of M3MP/Ph−TFVE are reported below: ^{1}H NMR (C_2D_6SO, 600 MHz): δ 7.43−7.31 (2H, Ar−H, t, J = 7.5 Hz), 7.21−7.18 (3H, Ar−H, dd, J = 15.3 Hz, 7.8 Hz), 6.65−6.55 (1H, CHF, d, J = 61.8), 3.64 (3H, CH_3, s), 3.16 (2H, CH_2, t, J = 6.9 Hz), 2.77 (2H, CH_2, t, J = 6.9 Hz), X = residual water (3.33) and residual C_2H_6SO (2.50). ^{19}F NMR (C_2D_6SO, ref $CF_3C_6H_5$, 565 MHz): δ −90.22 to −90.64 (1F, CF_2, ddd, J = 224.8 Hz, 11.7 Hz, 2.0 Hz), −92.00 to −92.42 (1F, CF_2, ddd, J = 225.0 Hz, 14.8 Hz, 5.7 Hz) −138.79 to −138.95 (1F, CHF, dt, J = 59.2 Hz, 14.3 Hz), X = $CF_3C_6H_5$. ^{13}C NMR (C_2D_6SO, 151 MHz): δ 171.3, 154.5, 130.0, 124.5, 116.8, 51.6, 34.5, 22.6.

4.3. Thiol−Alkene Model Reactions. Reactions between benzyl mercaptan and traditional alkene monomers were conducted in a similar fashion as the model reactions: benzyl mercaptan and an alkene monomer (5-norbornene-2-methanol (Norbornene), *n*-butyl vinyl ether (Vinyl Ether), allyl phenyl ether (Allyl Ether), methyl eugenol (Allyl), and phenyl trifluorovinyl ether (TFVE)) were combined in a 1:1 SH:alkene mole ratio along with 1 wt % Irgacure 1173. Reaction vessels were subjected to three cycles of freeze−pump−thaw and polymerized under 100 mW/cm^2 UV light for 30 min. Conversion was monitored via ^{1}H NMR and integration of the alkene peak.

4.4. Synthesis of Bisphenol a Bisallyl Ether (Allyl−BPA). Bisphenol A (15.00 g, 65.7 mmol) and potassium carbonate (22.7 g, 164.2 mmol) were dissolved in 75 mL of acetone before the addition of allyl bromide (19.88 g, 164.3 mmol). The reaction mixture was stirred overnight, followed by the removal of solvent under reduced pressure. The crude mixture was redissolved in 100 mL of CH_2Cl_2 and washed 3 × 100 mL with Na_2SO_4 solution and 1 × 100 mL with DI H_2O. The organic phase was separated and dried over $MgSO_4$, and solvent was removed via rotary evaporation. The crude oil was purified over a neutral alumina plug using neat petroleum ether as eluent to provide the product as a colorless oil. Isolated yield = 77%. ^{1}H NMR ($CDCl_3$, 600 MHz): δ 7.14 (4H, Ar−H, d, J = 6.6 Hz), 6.82 (4H, Ar−H, d, J = 6.7 Hz), 6.06 (2H, C<u>H</u>=CH$_2$, m), 5.35 (4H, CH=C<u>H</u>$_2$, dd, J = 80.3 Hz, 13.8 Hz), 4.52 (4H, CH_2, s), 1.65 (6H, CH_3, s). ^{13}C NMR ($CDCl_3$, 151 MHz): δ 156.2, 143.4, 133.7, 127.9, 117.6, 114.2, 68.9, 41.8, 31.2 (Figures S15 and S16).

4.5. Synthesis of 1,1-Bis[4-(2-bromo-1,1,2,2-tetrafluoroethoxy)]isopropylidene (BrE−BPA). BrE−BPA was synthesized according to a modified literature procedure.[11] BPA (15.00 g, 65.70 mmol) and Cs_2CO_3 (53.00 g, 162.6 mmol) were dissolved in 100 mL of DMSO under an inert atmosphere. The solution was brought to 50 °C, and 1,2-dibromotetrafluoroethane (43.60 g, 167.9 mmol) was added slowly to the heated mixture. The reaction was stirred overnight, followed by slow dilution with 100 mL of DI H_2O. The mixture was extracted 5 × 100 mL with petroleum ether, and the collected organic phase was washed 3 × 200 mL with DI H_2O. Following drying with Na_2SO_4, the solution was filtered and concentrated via rotary evaporation. The crude oil was further purified by silica gel chromatography using a 98:2 (v:v) petroleum ether:CH_2Cl_2 eluent. Chromatography returned a colorless oil. Yield = 63%. ^{1}H NMR ($CDCl_3$, 600 MHz): δ 7.26 (4H, Ar−H, d, J = 7.5 Hz), 7.16 (4H, Ar−H, d, J = 6.4 Hz), 1.72 (6H, CH_3, s). ^{19}F NMR ($CDCl_3$, ref $CF_3C_6H_5$, 565 MHz): δ −68.9 (2F, OCF_2CF_2Br, t, J = 4.8 Hz), −86.9 (2F, OCF_2CF_2Br, t, J = 4.7 Hz). ^{13}C NMR ($CDCl_3$, 151 MHz): δ 149.0, 147.0, 128.2, 121.3, 42.75, 31.0 (Figures S17−S19).

4.6. Synthesis of 1,1-Bis(4-trifluorovinyloxy)phenyl)-isopropylidene (TFVE−BPA). To a reaction flask fixed with a condenser was charged 100 mL of MeCN and 7.94 g (121.4 mmol) of zinc dust. The solution was brought to reflux and BrE−BPA (27.23 g, 46.46 mmol) was added slowly. The reaction was stirred overnight and cooled, and the mixture was vacuum filtered to remove residual zinc, followed by removal of MeCN under reduced pressure. The crude organic phase was dissolved in 50 mL of hexanes and filtered a second time to remove addition Zn salts. Hexanes was removed under reduced pressure, and the crude oil was purified by silica gel chromatography using 95:5 (v:v) petroleum ether:CH_2Cl_2 as an eluent to afford the pure product as a colorless oil. Isolated yield = 60%. ^{1}H NMR ($CDCl_3$, 600 MHz): δ 7.26 (4H, Ar−H, d, J = 7.2 Hz), 7.05 (4H, Ar−H, d, J = 6.9 Hz), 1.71 (6H, CH_3, s). ^{19}F NMR ($CDCl_3$, ref $CF_3C_6H_5$, 565 MHz): δ −121.0 (1F, C<u>F</u>$_2$=CF, dd, J = 97.6 Hz, 57.9 Hz), −127.8 (1F, C<u>F</u>$_2$=CF, dd, J = 109.7 Hz, 97.6 Hz), −134.6 (1F, CF$_2$=C<u>F</u>, dd, J = 109.6 Hz, 58.0 Hz). ^{13}C NMR ($CDCl_3$, 151 MHz): δ 153.4, 147.2, 128.4, 115.7, 42.4, 31.0 (Figures S20−S22).

4.7. Network Preparation. Trimethylolpropane tris(3-mercaptopropionate) (TMPMP) and 1,6-hexanedithiol (HexSH_2) were

DOI: 10.1021/acs.macromol.6b01822
Macromolecules 2016, 49, 7667−7675

combined in a 25:75 mol % SH ratio, along with 1 wt % Irgacure 1173. The alkene ratio was varied from 0:100 to 100:0 mol % TFVE−BPA: Allyl−BPA maintaining a 1:1 SH:alkene mole ratio. Formulations were then cast into various molds under air and inert atmosphere and polymerized for 30 min under a 365 nm centered UV light at an intensity of 40 mW/cm^2.

4.8. Characterization. Structural analysis of synthesized compounds was conducted using a Bruker Ascend 600 MHz spectrometer. Polymerization kinetic data were collected by real time FTIR (RT-FTIR) using a Nicolet 8700 spectrometer with a KBr beam splitter and a MCT/A detector. Samples were sandwiched between two NaCl salt plates in an N_2 atmosphere and polymerized under 20 mW/cm^2 UV light for 5 min. Scans were acquired at a rate of approximately 3 scans/s. Conversions were calculated by measuring the change in area under the thiol, allyl ether, and TFVE peaks. Dynamic mechanical analysis was performed using a TA Instruments Q800 dynamic mechanical analyzer in tension film mode. Samples were heated from −30 to 80 °C at a rate of 3 °C/min with a frequency amplitude of 15 μm. Mechanical testing was performed using a MTS Insight material testing machine equipped with a 2.5 kN load cell. Dog-bone samples were synthesized with approximate dimensions of 1.60 mm × 5.00 mm and a gauge length of 16.70 mm. Materials were deformed at a constant rate of 50 mm/min. Stress and strain at break were determined directly from the tensile test. Toughness was calculated by determining the area under the curve using the Integrate function in Origin 8.6 software, based on an average of at minimum three samples. Static contract angle measurements were performed using a Rame-Hart 200−00 Std.-Tilting B. goniometer. Static angles were measured using a 6 μL drop, and the average of three measurements is reported. Thermogravimetric analysis was conducted using a TA Instruments Q50 thermogravimetric analyzer with a platinum pan. Samples were equilibrated at 30.00 °C before ramping 10.00 °C/min to 800.00 °C under a nitrogen atmosphere with a flow rate of 10 mg/mL.

■ ASSOCIATED CONTENT

Supporting Information

The Supporting Information is available free of charge on the ACS Publications website at DOI: 10.1021/acs.macromol.6b01822.

NMR of synthesized compounds, structures of model alkenes, ^{19}F splitting patterns of M3MP/Ph−TFVE addition adduct, BnSH/Ph−TFVE small molecule kinetics, thiol−ene oxygen reaction mechanism, ^{19}F NMR of thiol/TFVE degradation products, and contact angle measurements of TFVE−BPA based polymer networks (Figures S1−S23) (PDF)

■ AUTHOR INFORMATION

Corresponding Author

*E-mail derek.patton@usm.edu (D.L.P.).

Notes

The authors declare no competing financial interest.

■ ACKNOWLEDGMENTS

The authors acknowledge partial financial support from the National Science Foundation (NSF DMR-1056817) and the American Chemical Society Petroleum Research Fund (PRF# 55833-ND7). B.R.D. thanks the US Dept. of Education GAANN Fellowship Program (Award #P200A120118) for financial support. J.E.B. was supported by the NSF REU program at the University of Southern Mississippi (DMR-1359239). Special thanks to Dr. Scott T. Iacono of the United States Air Force Academy for many enlightening conversations.

■ REFERENCES

(1) Maier, G. Low dielectric constant polymers for microelectronics. *Prog. Polym. Sci.* **2001**, *26* (1), 3−65.

(2) Liu, F.; Hashim, N. A.; Liu, Y.; Abed, M. R. M.; Li, K. Progress in the production and modification of PVDF membranes. *J. Membr. Sci.* **2011**, *375* (1−2), 1−27.

(3) Améduri, B.; Boutevin, B.; Kostov, G. Fluoroelastomers: synthesis, properties and applications. *Prog. Polym. Sci.* **2001**, *26* (1), 105−187.

(4) Cui, Z.; Drioli, E.; Lee, Y. M. Recent progress in fluoropolymers for membranes. *Prog. Polym. Sci.* **2014**, *39* (1), 164−198.

(5) Scheirs, J. *Modern Fluoropolymers*; Wiley: New York, 1997.

(6) Iacono, S. T.; Budy, S. M.; Jin, J.; Smith, D. W. Science and technology of perfluorocyclobutyl aryl ether polymers. *J. Polym. Sci., Part A: Polym. Chem.* **2007**, *45* (24), 5705−5721.

(7) Babb, D. A.; Ezzell, B. R.; Clement, K. S.; Richey, W. F.; Kennedy, A. P. Perfluorocyclobutane aromatic ether polymers. *J. Polym. Sci., Part A: Polym. Chem.* **1993**, *31* (13), 3465−3477.

(8) Jin, J.; Iacono, S. T.; Smith, D. W. Semifluorinated Polymers from Trifluorovinyl Aromatic Ether Monomers. In *Handbook of Fluoropolymer Science and Technology*; John Wiley & Sons, Inc.: Hoboken, NJ, 2014; pp 343−361.

(9) Jin, J. Chemistry of Aryl Trifluorovinyl Ethers. *Chemistry in New Zealand* **2012**, *76*, 24−26.

(10) Rico, I.; Wakselman, C. Condensation of 1,2-dibromotetrafluoroethane with Various Potassium Thiophenoixdes and Phenoxides. *J. Fluorine Chem.* **1982**, *20*, 759−764.

(11) Li, J.; Qiao, J. X.; Smith, D.; Chen, B.-C.; Salvati, M. E.; Roberge, J. Y.; Balasubramanian, B. N. A practical synthesis of aryl tetrafluoroethyl ethers via the improved reaction of phenols with 1,2-dibromotetrafluoroethane. *Tetrahedron Lett.* **2007**, *48* (42), 7516−7519.

(12) Brown, D. K.; Iacono, S. T.; Cracowski, J.-M.; Christensen, K.; Smith, D. W. Synthesis and characterization of a biphenyl perfluorocyclobutyl (BP-PFCB) polyethylene glycol (PEG) blend compatibilizer. *Polym. Adv. Technol.* **2016**, *27*, 1389−1396.

(13) He, F.; Gao, Y.; Jin, K.; Wang, J.; Sun, J.; Fang, Q. Conversion of a Biorenewable Plant Oil (Anethole) to a New Fluoropolymer with Both Low Dielectric Constant and Low Water Uptake. *ACS Sustainable Chem. Eng.* **2016**, *4*, 4451−4456.

(14) Wang, J.; Jin, K.; Sun, J.; Fang, Q. Dendrimeric organosiloxane with thermopolymerizable -OCF═F2 groups as the arms: synthesis and transformation to the polymer with both ultra-low k and low water uptake. *Polym. Chem.* **2016**, *7* (20), 3378−3382.

(15) Wong, S.; Ma, H.; Jen, A. K. Y.; Barto, R.; Frank, C. W. Highly Fluorinated Trifluorovinyl Aryl Ether Monomers and Perfluorocyclobutane Aromatic Ether Polymers for Optical Waveguide Applications. *Macromolecules* **2003**, *36* (21), 8001−8007.

(16) Smith, D. W.; Babb, D. A. Perfluorocyclobutane Aromatic Polyethers. Synthesis and Characterization of New Siloxane-Containing Fluoropolymers. *Macromolecules* **1996**, *29* (3), 852−860.

(17) Liu, S.; Jiang, X.; Ma, H.; Liu, M. S.; Jen, A. K. Y. Triarylamine-Containing Poly(perfluorocyclobutane) as Hole-Transporting Material for Polymer Light-Emitting Diodes. *Macromolecules* **2000**, *33* (10), 3514−3517.

(18) Ma, H.; Wu, J.; Herguth, P.; Chen, B.; Jen, A. K. Y. A Novel Class of High-Performance Perfluorocyclobutane-Containing Polymers for Second-Order Nonlinear Optics. *Chem. Mater.* **2000**, *12* (5), 1187−1189.

(19) Klukovich, H. M.; Kean, Z. S.; Iacono, S. T.; Craig, S. L. Mechanically Induced Scission and Subsequent Thermal Remending of Perfluorocyclobutane Polymers. *J. Am. Chem. Soc.* **2011**, *133* (44), 17882−17888.

(20) Zhu, Y.; Huang, Y.; Meng, W.-D.; Li, H.; Qing, F.-L. Novel perfluorocyclobutyl (PFCB)-containing polymers formed by click chemistry. *Polymer* **2006**, *47* (18), 6272−6279.

(21) Harris, J. F.; Stacey, F. W. The free radical addition of trifluoromethanethiol to fluoroolefins. *J. Am. Chem. Soc.* **1961**, *83*, 840−845.

DOI: 10.1021/acs.macromol.6b01822
Macromolecules 2016, 49, 7667−7675

(22) Harris, J. F. The free radical addition of hydrogen sulfide to fluoroethylenes. *J. Am. Chem. Soc.* **1962**, *84*, 3148−3153.
(23) Hoyle, C. E.; Bowman, C. N. Thiol-ene Click Chemistry. *Angew. Chem., Int. Ed.* **2010**, *49*, 1540−1573.
(24) Lowe, A. B. Thiol-ene "click" reactions and recent applications in polymer and materials synthesis: a first update. *Polym. Chem.* **2014**, *5* (17), 4820−4870.
(25) Xiong, L.; Kendrick, L. L.; Heusser, H.; Webb, J. C.; Sparks, B. J.; Goetz, J. T.; Guo, W.; Stafford, C. M.; Blanton, M. D.; Nazarenko, S.; Patton, D. L. Spray-Deposition and Photopolymerization of Organic−Inorganic Thiol−ene Resins for Fabrication of Super-amphiphobic Surfaces. *ACS Appl. Mater. Interfaces* **2014**, *6* (13), 10763−10774.
(26) Lin, H.; Wan, X.; Jiang, X.; Wang, Q.; Yin, J. A "thiol-ene" photo-curable hybrid fluorinated resist for the high-performance replica mold of nanoimprint lithography (NIL). *J. Mater. Chem.* **2012**, *22* (6), 2616−2623.
(27) Sangermano, M.; Bongiovanni, R.; Malucelli, G.; Priola, A.; Harden, A.; Rehnberg, N. Synthesis of new fluorinated allyl ethers for the surface modification of thiol−ene ultraviolet-curable formulations. *J. Polym. Sci., Part A: Polym. Chem.* **2002**, *40* (15), 2583−2590.
(28) D'Souza, V. T.; Nanjundiah, R.; Baeza, J.; Szmant, H. H. Thiol-Olefin Cooxidation (TOCO) Reaction. 7. A ^{1}H NMR Study of Thiol Solvation. *J. Org. Chem.* **1987**, *52* (9), 1720−1725.
(29) Antonucci, J. M. The Synthesis and Polymerization of Fluorostyrenes and Fluorinated Vinyl Phenyl Ethers. In *Fluoropolymers*; Wall, L. A., Ed.; John Wiley & Sons, Inc.: New York, 1972; pp 33−82.
(30) Cramer, N. B.; Scott, J. P.; Bowman, C. N. Photopolymerizations of thiol−ene polymers without photoinitiators. *Macromolecules* **2002**, *35* (14), 5361−5365.
(31) Cirkva, V.; Polák, R.; Paleta, O. Radical additions to fluoroolefins. Photochemical fluoroalkylation of alkanols and alkane diols with perfluoro vinyl ethers; photo-supported O-alkylation of butane-1,4-diol with hexafluoropropene. *J. Fluorine Chem.* **1996**, *80* (2), 135−144.
(32) Timperley, C. M. Fluoroalkene chemistry: Part 2. Reactions of thiols with some toxic 1,2-dichlorinated polyfluorocycloalkenes. *J. Fluorine Chem.* **2004**, *125* (9), 1265−1272.
(33) O'Brien, A. K.; Cramer, N. B.; Bowman, C. N. Oxygen inhibition in thiol−acrylate photopolymerizations. *J. Polym. Sci., Part A: Polym. Chem.* **2006**, *44* (6), 2007−2014.
(34) Rabek, J. F., Photochemical aspects of degradtion of polymers. In *Polymer Photodegradation*; Springer: Netherlands, 1995; pp 24−66.
(35) Chiantore, O.; Trossarelli, L.; Lazzari, M. Photooxidative degradation of acrylic and methacrylic polymers. *Polymer* **2000**, *41* (5), 1657−1668.
(36) Herman, M. F. *Encyclopedia of Polymer Science and Technology*, 3rd ed.; Wiley: Hoboken, NJ, 2007.
(37) Yuan, Y.; Shoichet, M. S. Insights into the Properties of Novel Trifluorovinyl Ether Copolymers. *Macromolecules* **1999**, *32*, 2669−2674.
(38) Dargaville, T. R.; George, G. A.; HIll, D. J. T.; Scheler, U.; Whittaker, A. K. High-speed MAS 19F NMR Analysis of an Irradiated Fluoropolymer. *Macromolecules* **2002**, *35*, 5544−5549.
(39) Lappan, U.; Geißler, U.; Scheler, U.; Lunkwitz, K. Identification of new chemical structures in poly(tetrafluoroethylene-co-perfluoropropyl vinyl ether) irradiated in vacuum at different temperatures. *Radiat. Phys. Chem.* **2003**, *67* (3−4), 447−451.
(40) Cohen, O.; Sasson, R.; Rozen, S. A new method for making acyl fluorides using BrF3. *J. Fluorine Chem.* **2006**, *127* (3), 433−436.
(41) Nguyen, T.; Wakselman, C. A new route to perfluorinated sulphonic acid resin intermediates. *Eur. Polym. J.* **1991**, *27* (4), 435−438.
(42) Ciampelli, F.; Venturi, M. T.; Sianesi, D. The 19F chemical shift in oxygen containing carbon fluorine products. *Org. Magn. Reson.* **1969**, *1*, 281−293.
(43) Henry, D. J.; Parkinson, C. J.; Mayer, P. M.; Radom, L. Bond Dissociation Energies and Radical Stabilization Energies Associated with Substituted Methyl Radicals. *J. Phys. Chem. A* **2001**, *105* (27), 6750−6756.
(44) Hoyle, C. E.; Lee, T. Y.; Roper, T. Thiol−enes: Chemistry of the past with promise for the future. *J. Polym. Sci., Part A: Polym. Chem.* **2004**, *42* (21), 5301−5338.
(45) Teng, H. Overview of the Development of the Fluoropolymer Industry. *Appl. Sci.* **2012**, *2*, 496−512.
(46) Rigby, H. A.; Bunn, C. W. A Room-Temperature *T*ransition in Polytetrafluoroethylene. *Nature* **1949**, *164*, 583−585.
(47) Boufflet, P.; Han, Y.; Fei, Z.; Treat, N. D.; Li, R.; Smilgies, D.-M.; Stingelin, N.; Anthopoulos, T. D.; Heeney, M. Using molecular design to increase hole transport: Backbone fluorination in the benchmark material poly(2,5-bis(3-alkylthiophen-2-yl)thieno[3,2-***b***-]-thiophene (pBTTT). *Adv. Funct. Mater.* **2015**, *25*, 7038−7048.
(48) Moody, J. D.; VanDerveer, D.; Smith, D. W., Jr.; Iacono, S. T. Synthesis of Internal Fluorinated Alkenes via Facile Aryloxylation of Substituted Phenols with Aryl Trifluorovinyl Ethers. *Org. Biomol. Chem.* **2011**, *9*, 4842−4849.
(49) Alkorta, I.; Rozas, I.; Elguero, J. Effects of fluorine substitution on hydrogen bond interactions. *J. Fluorine Chem.* **2000**, *101* (2), 233−238.
(50) Paul, A.; Griffiths, P. C.; James, R.; Willock, D. J.; Rogueda, P. G. Explaining the phase behaviour of the pharmaceutically relevant polymers poly(ethylene glycol) and poly(vinyl pyrrolidone) in semi-fluorinated liquids. *J. Pharm. Pharmacol.* **2005**, *57* (8), 973−980.
(51) Kwei, T. K. The effect of hydrogen bonding on the glass transition temperatures of polymer mixtures. *J. Polym. Sci., Polym. Lett. Ed.* **1984**, *22* (6), 307−313.
(52) Hayashi, M.; Noro, A.; Matsushita, Y. Highly extensible supramolecular elastomers with large stress generation capability originating from multiple hydrogen bonds on the long soft network strands. *Macromol. Rapid Commun.* **2016**, *37* (8), 678−684.
(53) Zulfiqar, S.; Zulfiqar, M.; Rizvi, M.; Munir, A.; McNeill, I. C. Study of the thermal degradation of polychlorotrifluoroethylene, poly(vinylidene fluoride) and copolymers of chlorotrifluoroethylene and vinylidene fluoride. *Polym. Degrad. Stab.* **1994**, *43* (3), 423−430.

DOI: 10.1021/acs.macromol.6b01822
Macromolecules 2016, 49, 7667−7675